古 脊 椎 动 物 学 报
VERTEBRATA PALASIATICA

DOI: 10.19615/j.cnki.2096-9899.240123

First report of *Hispanodorcas* from the Late Miocene of China

WU Yong[1] WANG Shi-Qi[2*] LIANG Zhi-Yong[1] GUO Ding-Ge[2,3]
SUN Bo-Yang[2] LIU Long[1] DUAN Kai[1] CHEN Guo-Zhong[1]

(1 *The Third Geological and Mineral Exploration Institute of Gansu Bureau of Geology and Mineral Resources* Lanzhou 730050)
(2 *Key Laboratory of Vertebrate Evolution and Human Origins of Chinese Academy of Sciences*, *Institute of Vertebrate Paleontology and Paleoanthropology*, *Chinese Academy of Sciences* Beijing 100044)
(3 *University of Chinese Academy of Sciences* Beijing 100049)
* Corresponding author: wangshiqi@ivpp.ac.cn

Abstract As a small to middle-sized bovid, *Hispanodorcas* had previously only been found in the pan-Mediterranean region and South Asia. Its taxonomic classification at the tribe level has been a subject of debate, with possible associations to Antilopini, Reduncini, or Oiocerini. Here, we report on the first discovery of *Hispanodorcas* in East Asia, *H. longdongica* sp. nov. from the Daidian Locality in China, dating to the early Baodean age (~8–7 Ma). The new material consists of five skulls with varying states of preservation and provides the most complete osteological information on *Hispanodorcas* to date. It features a long, slender, and posteriorly curved horncore with a weak homonymous twist and both laterodorsal and medioventral grooves, which is characteristic of *Hispanodorcas*. This new species is characterized by having the smallest size amongst all known *Hispanodorcas* species, a weakly curved brain case in the facial region, and poorly developed posterior and anterior basilar tuberosities. These primitive characteristics suggest that *H. longdongica* may represent an early evolutionary stage of this genus. Furthermore, they indicate that *Hispanodorcas* might have directly evolved from the *Gazella* stock. The homonymous twist in the horncore, which aligns with Oiocerini, may be a case of homoplasy.

Key words Qingyang, East Asia, Baodean, Antilopini, *Hipparion* fauna, *Hispanodorcas*

Citation Wu Y, Wang S Q, Liang Z Y et al., in press. First report of *Hispanodorcas* from the Late Miocene of China. Vertebrata PalAsiatica. DOI: 10.19615/j.cnki.2096-9899.240123

1 Introduction

Hispanodorcas is a small to middle-sized *Gazella*-like bovid, which lived during the Late Miocene and Early Pliocene periods (Thomas et al., 1982; Bouvrain and de Bonis, 1988; Alcalá and Morales, 2006; Kostopoulos, 2014). It is characterized by a pair of horncores that exhibit a weak homonymous twist (the left horn core twisting clockwise in distal view). Consequently, the taxonomic classification of this animal remains somewhat controversial, with suggestions

国家重点研发计划 (No. 2023YFF0804500)、第二次青藏科考(2019QZKK0705)和甘肃省级古生物化石保护项目资助。
收稿日期：2023-11-13

including Antilopini, Reduncini, and Oiocerini. *Hispanodorcas* has been discovered in Europe (Spain and Greece) and South Asia (Pakistan) (Raza et al., 2002; Kostopoulos, 2014), but it has not yet been reported in the eastern part of Eurasia, including China.

In 2021, The Third Geological and Mineral Exploration Institute of Gansu Bureau of Geology and Mineral Resources organized fossil excavations at the Daidian locality of Qingyang City, Gansu Province, Western China (Fig. 1A), resulting in the recovery of an abundance of fossil mammals. Our preliminary identification has led to the discovery of 18 taxa, including *Adcrocuta eximia*, Hyaenidae gen. et sp. indet., Mustelidae gen. et sp. indet., *Paratetralophodon* ? sp., *Hipparion hippidiodus*, *Hi. coelophyes*, *Acerorhinus* sp., Rhinoceratini gen. et sp. indet., *Chleuastochoerus stehlini*, *Schansitherium tafeli*, *Samotherium* ? sp. *Palaeotragus* ? sp. Cervidae gen. et sp. indet., Moschidae gen. et sp. indet., *Gazella paotehensis*, *G. gaudryi*, *Hispanodorcas longdongica* sp. nov., and Bovidae gen. et sp. indet. These taxa characterize the "*Hipparion*" fauna of the Late Miocene in northern China (Flynn et al., 2011; Sun et al., 2022). Among these taxa *Hi. hippidiodus* and *Hi. coelophyes* seem to be present in areas more commonly associated with the early Baodean Age (Sun, 2018, 2023). Based on our estimation, the age of the Daidian assemblage is ~8–7 Ma. Of particular interest is the discovery of the most well-preserved *Hispanodorcas* material to date, which includes five more or less complete skulls, one of which is associated with a mandible. This population of *Hispanodorcas*, displays relatively primitive morphology compared to other species within the genus. The new *Hispanodorcas* material has significant importance in regards to enhancing our understanding of the evolutionary history of this intriguing bovid.

2 Geological settings

The Daidian fossil assemblage was discovered near the Daidian township, which is in the district of the Zhengning County of Qingyang City, Gansu Province (Fig. 1A). The Neogene strata in the Qingyang Region unconformably overlay the Mesozoic base, the Early Cretaceous Jingchuan Formation, which is composed of reddish sandstones intercalated with mudstones and shales. These Neogene strata are characterized by reddish or brownish mudstones and silty mudstones interbedded with carbonated nodules, indicating a high degree of pedogenesis. They also contain an abundance of fossil mammals known as the "*Hipparion* Fauna" (Flynn et al., 2011; Sun et al., 2022). Quaternary strata, represented by aeolian deposits, have unconformably eroded the Neogene strata, creating several layers of alluvial sandy pebble stones.

Daidian Section (35°18′38.29″N, 108°11′37.36″E) (Fig. 1B, C):

Late Pleistocene Malan Formation

13. light yellowish incompact loess, based on a layer of paleosols 5.8 m

----------parallel unconformity----------

Early Pleistocene Sanmen Formation

12. brownish yellow sandy mudstones or sandy clays 3.85 m

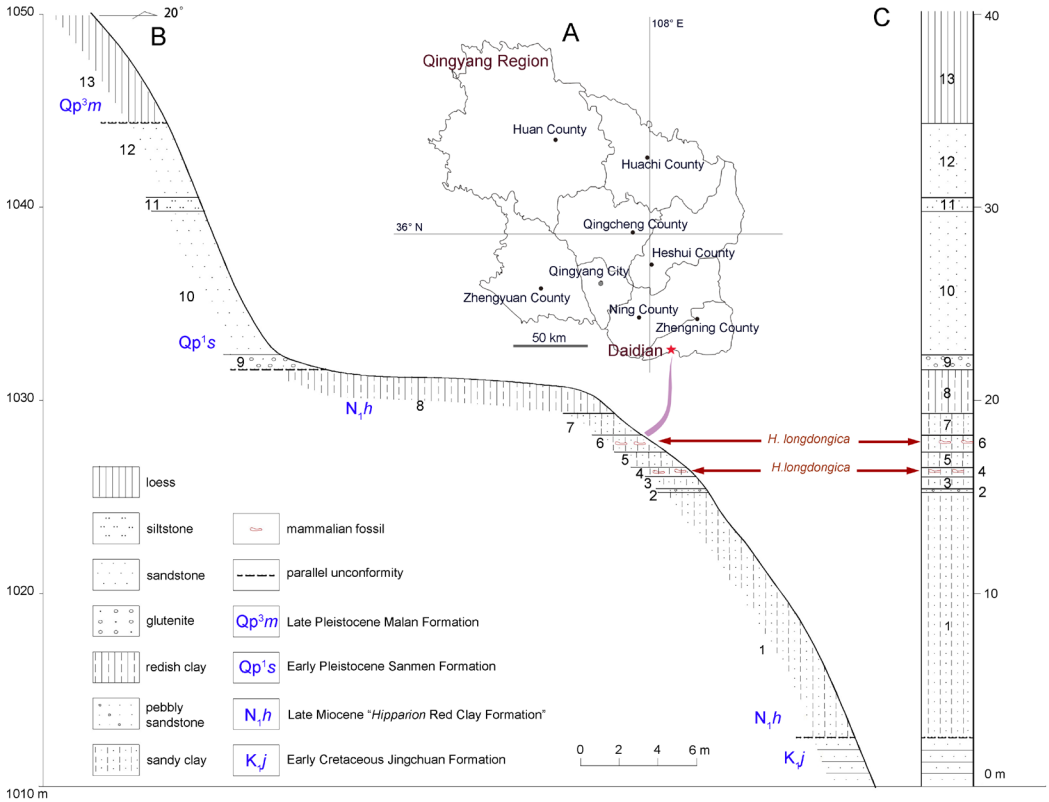

Fig. 1 Locator map of the fossil site of *Hispanodorcas* (A), the section (B), and the stratigraphic column of Daidian locality (C), from which *H. longdongica* was produced

11. light yellowish with slightly reddish thin-bedded silty stones 0.72 m
10. yellowish fine-grained sandy clays 7.43 m
9. fine-grained pebble stones intercalated with lenses of coarse-grained sandstones, bearing large-scaled clinostratified cross-beddings 0.77 m

----------parallel unconformity----------

Late Miocene "*Hipparion* Red Clay Formation"

8. light reddish compact loess with micro-horizontal beddings, based on a layer of carbonated nodules and fine pebbles 2.27 m
7. light brownish red silty clays 1.12 m
6. light grayish orange horizontostratified silty clays, bearing mammalian fossils: *Hippotherium weihoense*, *Hipparion hippidiodus*, *Hi. coelophyes*, *Schansitherium tafeli*, *Gazella gaudryi*, *Hispanodorcas longdongica* sp. nov. 0.88 m
5. light grayish orange silty clays 0.8 m
4. light grayish orange horizontostratified silty clays, bearing mammalian fossils 0.48 m
3. light grayish orange silty clays 0.62 m
2. light reddish silty clays containing pebbles 0.05 m
1. light reddish silty clays 12.7 m

~~~~~~~~~~~~~ angular unconformity ~~~~~~~~~~~~~

Early Cretaceous Jingchuan Formation

0. reddish sandstones intercalated with mudstones and shales not to bottom

3 Materials and methods

All the specimens described in the present paper were housed in the Gansu Geological Museum (GGM GSYK), Lanzhou, China. The cheek teeth terminology follows Bärmann and Rössner (2011). The cranial and mandibular measurements follow Bärmann et al. (2013). Linear measurements were taken using calipers and angular measurements were taken using photos.

Anatomical abbreviations at, acoustic tube; Et, eustachian tube; Ev, ethmoidal vacuity; fc, fenestra cochleae; f cs, facial sulcus; f g, glenoid fossa; f h, hypoglossal foramina; f L, lacrimal fossa; f o, foramen oval; f pc, post-cornual fossa; f pg, postglenoid foramen; f ro, foramen rotundum; f sm, stapedial muscle fossa; f so, supraorbital foramen; f tt, temsor tympani; l o, lacrimal orifice; M, mastoid; Ob, orbit; of, optical foramen; Op, occipital protuberance; pr, promontorium; s Fm, frontal median suture; s F-P, suture between frontal and parietal; s N-F, suture between nasal and frontal; t ab, anterior basilar tuberosity; tb, tympanic bulla; tl, temporal line; t pb, posterior basilar tuberosity; tv, tympanohyal vagina.

4 Systematic paleontology

Family Bovidae Gray, 1821

Subfamily Antilopinae Gray, 1821

***Hispanodorcas* Thomas et al., 1982**

***Hispanodorcas Longdongica* sp. nov.**

(Figs. 2, 4, 5; Tables 1–4)

The taxon *Hispanodorcas longdongica* has been registered in ZOOBANK: http://zoobank.org/ B8074A45-AB1B-4D44-850A-A4119565FD37.

Type Species *H. torrubiae* Thomas et al., 1982.

Included species *H. orientalis* Bouvrain and de Bonis, 1988; *H. heintzi* Alcalá and Morales, 2006; *H. longdongica* sp. nov.

Holotype GGM GSKY 22010, cranium bearing the horncore pair, facial part missing.

Etymology the species name derives from the region name, Longdong, where the new specimens were discovered.

Referred specimens GGM GSKY 22011, cranium lacking horncores, the braincase and rostrum more or less incomplete, P2–M3 tooth row present; GGM GSKY 22012, cranium fragment, distal horncores, most of the braincase missing; GGM GSKY 22013, juvenile cranium, and mandible bearing DP2–M2 and dp2–m2, horncores and caudal part of braincase broken; GGM GSKY 22014, dorsal part of cranium bearing the horncore pair.
~~~~~~~~~~~~~

Due to the fact that at least five middle to small-sized ruminants coexisted (*Gazella gaudryi*, *Gazella* sp., Cervidae indet., and Moschidae indet.), the post-cranium bones of *H. longdongica* will be reported on further after a comprehensive study of the assemblage.

Diagnosis *Hispanodorcas* of small size (size close to living Oribi, *Ourebia ourebi*); horncore long and slender, posteriorly curved, slightly diverge, moderately compressed, with a weak homonymous twist (1/2 circle); laterodorsal and medioventral grooves present (with variation); post cornual fossa round and deep, supraorbital foramen oval and deep. Cranial bent weak, resulting in a small angle between the horncore and dorsal cranium; occiput low; basioccipital and basisphenoid thin with relatively weak posterior and anterior basilar tuberosities. Tympanic bullae large, ellipsoid, with poorly developed lamina vaginalis; lacrimal fossa shallow, poorly defined. Cheek teeth high-crowned, lacking ecto/entostylies.

Differential diagnosis differing from *H. torrubiae*, *H. orientalis* and *H. heintzi* in the smaller size with the higher compression of horncores; further from *H. heintzi* in lacking an anterior keel of the horncores, and from *H.* cf. *H. orientalis* and *H. torrubiae* in the more posteriorly curved horncores; also differing from *H. orientalis* in the more posteriorly incline of the horncores (smaller angle between the horncores and the cranial roof); additionally, molars differing from *H. torrubiae* in the stronger buccal styles and smoother surfaces without enamel wrinkles (the latter character is only known from an M1, see Thomas et al., 1982).

Locality, horizon, and age Daidian (35°18′38.29″N, 108°11′37.36″E), belonging to the Zhengning County of the Qingyang City, Gansu Province (Fig. 1A); derived from the "*Hipparion* Red Clay Formation", Late Miocene, estimating ~8–7 Ma.

5 Description

Skull Horncore (Fig. 2) The horncores are long and slender, taper distally, and exhibit a slight divergence at an angle of approximately 30°. They are strongly posteriorly inclined because of the poorly bent braincase from the face. Among the horncores, the left horncore of the type specimen is the longest one, measuring 101.8 mm on the anterior edge, which is smaller than any complete horncore of the other species (Fig. 3A). All horncores exhibit a slow homonymous twist (the right horncore rotates anti-clockwise in distal view), approximately completing a semicircle. Proximally, the horncores are laterally compressed and gradually become dorsoventrally compressed distally. The proximal compression is more pronounced than that observed in other *Hispanodorcas* species (Fig. 3A, B), though no clear keel is developed (Fig. 2B). Longitudinal grooves are present throughout the horncore with two prominent ones. One of these grooves, the laterodorsal groove, may originate from the middle of the lateral side at the horncore base. It then extends throughout its entire length and gradually turns to the dorsal side distally in conjunction with the slight twist of the horncore (Fig. 2A1, B1, C1, blue color). The other prominent one, the ventromedial groove, may begin from the distal 1/2–2/3 of the horncore and then appears on the opposite side of the laterodorsal

groove (Fig. 2A3, B3, C3, green color). However, the development of the two grooves is variable. For example, in the type specimen, the laterodorsal and ventromedial grooves on both horncores are rather weak (Fig. 2A1, A3). In contrast, in the specimen GGM GSKY22014, the ventromedial grooves of both horncore, as well as the left laterodorsal groove, are well-defined (Fig. 2B1, B3, C3), while the right laterodorsal groove is almost absent (Fig. 2C1). The horncore bases are short and difficult to recognize from the horncore proper due to it lacking a sharp flange. The horncore insertion is near the dorsocaudal border of the orbit, and the distance between the two horncore bases is relatively wide (Fig. 4A–C). Additionally, a small, round post-cornual fossa is deeply excavated at the caudolateral corner of the horncore base (Fig. 4A3, C2, D2, f pc).

Fig. 2 Horncore of *Hispanodorcas longdongica* from Daidian Locality, Qingyang
A. left horncore of GGM GSKY 22010, the type specimen, in lateral (A1), anterior (A2), and median (A3) views; B, C. left (B) and right (C, images inversed) horncores of GGM GSKY 22014, in lateral (B1, C1), anterior (B2, C2), and median (B3, C3) views. The cross-sections are at 0, 40, and 70 mm from the horncore base. The blue and green shadows indicate the lateral and median grooves, respectively

Table 1 Horncore measurements of *Hispanodorcas longdongica*, from Daidian Locality , Qingyang (mm)

		anterior length	at base			at 70 mm		
			DAP	DT	DAP/DT (%)	DAP	DT	DAP/DT (%)
GSKY 22010	l	101.8	24.0 c. a.	18.0	75.0	12.4	8.3	66.9
	r	98.0	23.4	17.6	75.2	10.2	7.5	73.5
GSKY 22014	l	77.0 c. a.	19.0	14.4	75.8	7.5	4.1	54.7
	r	75.0 c. a.	19.1	14.5	75.9	—	—	—
GSKY 22012	l	—	20.9	14.4	68.9	—	—	—
	r	—	19.5	15.1	77.4	—	—	—

Abbreviations: DAP. anteroposterior diameter of horncore; DT. transversal diameter of horncore; l. left; r. right.

Braincase and cranial roof The braincase takes on an ellipsoid shape and is slightly inclined from the facial part at an angle of approximately 30° (Fig. 4A1). In dorsal view, the braincase exhibits notable width in comparison with the living gazelles (Fig. 4C1). The frontal bones that rise between the two horncores are restricted along the middle suture, which indicates the presence of a poorly developed frontal sinus (Fig. 4B, C1). The supraorbital

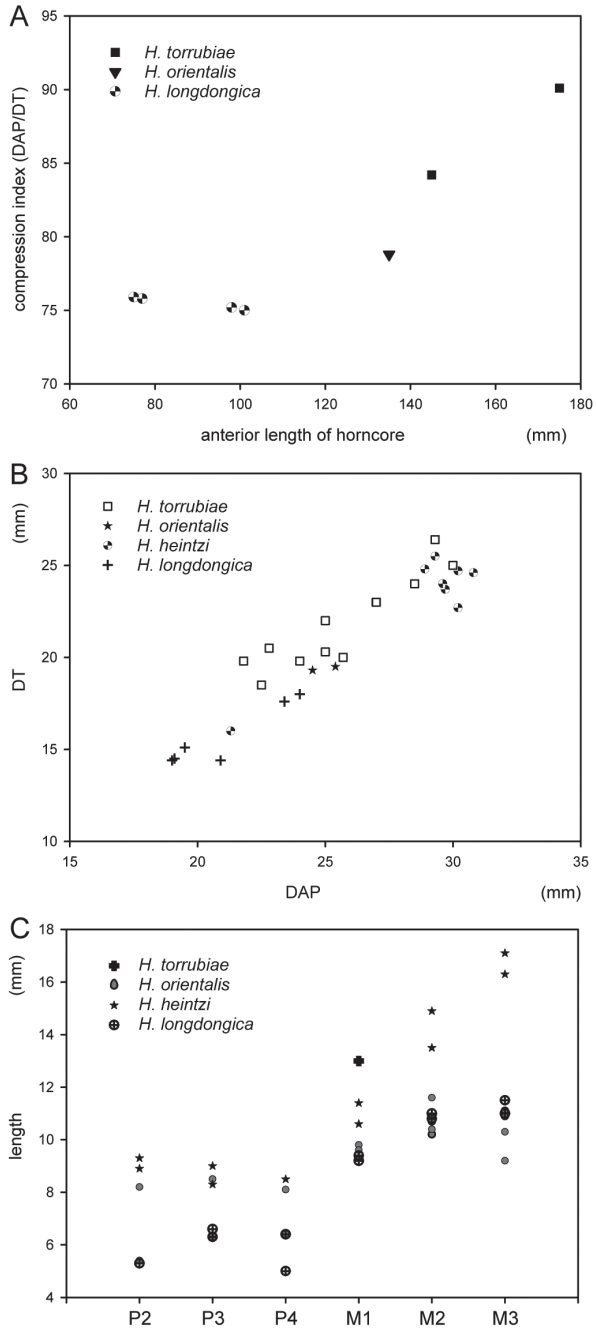

Fig. 3 Size comparisons of *Hispanodorcas* species

A. bivariate plot of anterior horn length and horncorn compression index;

B. bivariate plot of horncore DAP and DT; C. comparison of upper check tooth lengths

Abbreviations: DAP. anteroposterior diameter of horncore; DT. transversal diameter of horncore

foramen is vertically elliptical, deeply excavating the anteromedial root of the horncore base, and holds a small orifice (Fig. 4B, f so). The frontal median suture and the frontoparietal sutures are highly indented (Fig. 4C1, s Fm, s F-P). The parietal bone is relatively long, resulting in a large distance between frontoparietal and parietooccipital sutures. While the temporal lines are not distinctly defined, they present a considerable separation (Fig. 4C1, tl). In lateral view, the temporal crest horizontally divides the braincase and linkes anteriorly to the zygomatic process of squamosal bone (Fig. 4A1). On the dorsal side of the zygomatic process root, there is a deep fossa that is penetrated by the postglenoid foramen (Fig. 4D1, f pg).

Nuchal region In caudal view, the occiput is wide and low. The robust nuchal crest passes horizontally. In the center of the nuchal crest, there is an inverted triangular occipital protuberance (Fig. 4A3, Op) with a vertical crest that extends to the dorsal border of the foramen magnum. The condyles are sub-quadrate in shape, featuring a sharp ventral angle and encircling a sub-circular foramen magnum. The mastoid bone on the occipital surface is large (Fig. 4A3, M). The condyloid fossa is oval and deep. The development of hypoglossal foramina varies (Fig. 4A1, f h). For example, in the type specimen, there is only a very large right foramen and a moderately sized left one, which are accompanied by several small accessory foramina.

Facial region In dorsal view, the facial part anterior to the orbit is contracted (Fig. 4B, C1). The proximal ends of the nasal bones are at the level of the anterior orbital rim (Fig. 4B,

Table 2 cranial measurements of *Hispanodorcas longdongica* from Daidian Locality, Qingyang (mm)

Measurements	GGM GSKY 22010		GGM GSKY 22014		GGM GSKY 22011		GGM GSKY 22012		GGM GSKY 22013	
	Left/ median	right	Left/ median	right	Left/ median	right	Left/ median	right	Left/ median	right
Bulla length	19.2	20.7								
Bulla width	14.6	13.5								
Distance between horn pedicles		30.0	33.6				33.2			
Distance, orbit to condyle (measured parallel to tooth row)	83.3									
Distance between supra-orbital foramina					30.3					
Horn base distance (distance of the anterior-most parts of the pedicles)		32.8					46.6			
Inter-bullae distance		11.5								
Length of frontal + parietal					73.3				69.1?	
Length of basioccipital (at sagittal plane)		28.7								
Length of frontal					44.2					
Length of parietal					30.3				27.6	
Orbit diameter (parallel to tooth row)	38.9				30.9	34.9			31.7	32.7
Occipital height, braincase complete		28.6								
Width across orbits (maximum width of frontals)					71.6					
Width of braincase		54.4								
Width of basioccipital anterior		12.6			12.6					
Width of basioccipital posterior		17.4			16.8					
Width of condyle		34.7								
Width of palate, measured at level of palatal foramina					24.7				16.1	

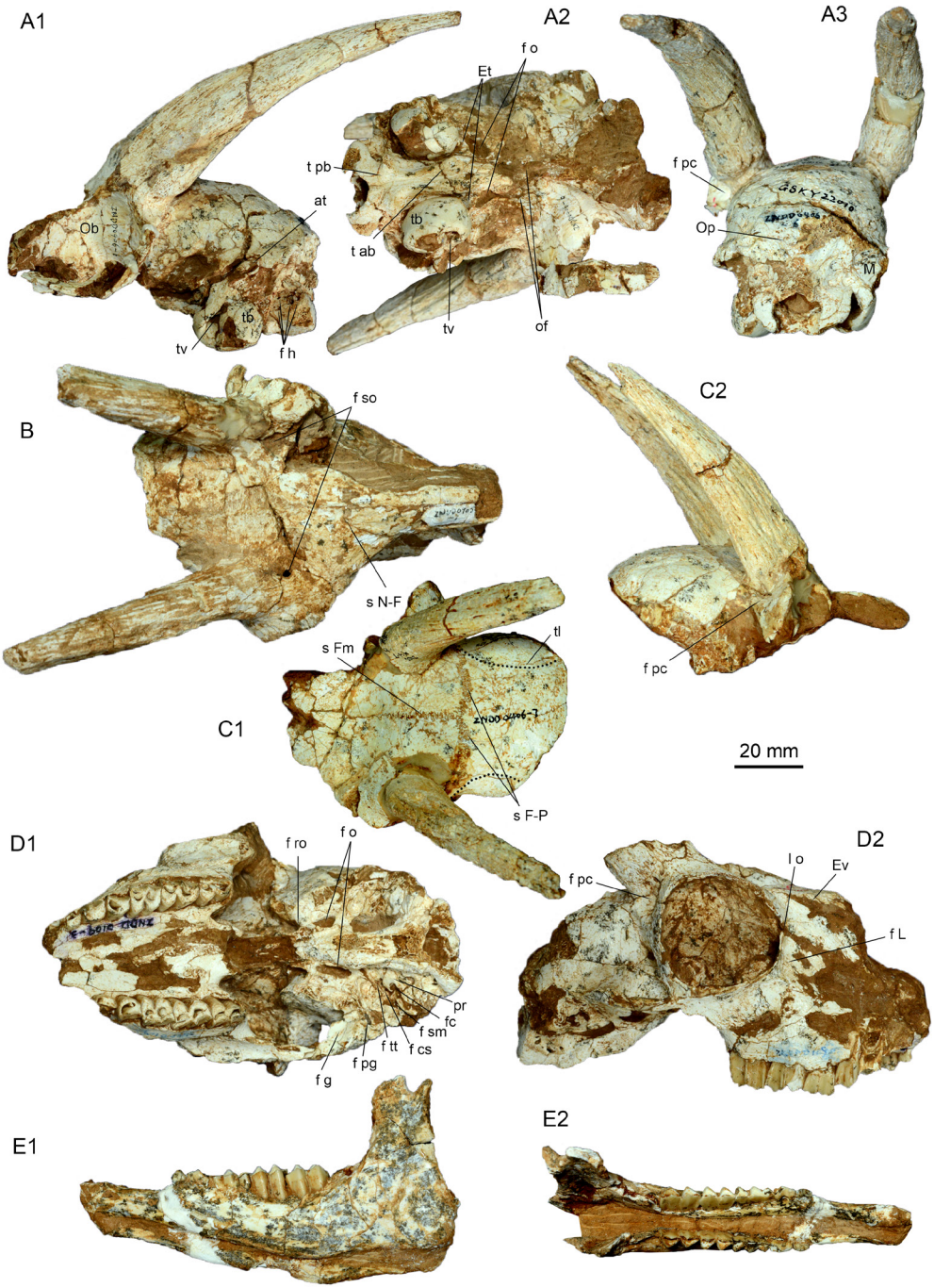

Fig. 4 Cranium (A−D) and mandible (E) of *Hispanodorcas longdongica* from Daidian Locality, Qingyang
A. GGM GSKY 22010, the type specimen, in lateral (A1), ventral (A2), and caudal (A3) views;
B. GGM GSKY 22012, in dorsal view; C. GGM GSKY 22014, in dorsal (C1) and lateral (C2) views;
D. GGM GSKY 22011, in ventral (D1) and lateral (D2) views;
E. GGM GSKY 22013, in lateral (E1) and occlusal (E2) views
For abbreviations, see the material and methods part

s N-F). In lateral view, a slit-like ethmoidal vacuity seems to be present (Fig. 4D2, Ev), but it is not very clear due to the high degree of breakage in this area. A shallow lacrimal fossa is present, but it is poorly defined (Fig. 4D2, f L) due to the weakly developed facial crest. The facial part ventral to the facial crest is convex and low. None of the premaxillary bones are well preserved. The infraorbital foramen is small and positioned at the level of the first cheek tooth. The palatine foramina, as well as the palatomaxillary suture, are damaged in all the specimens. The lateral palatal notch is deeper than the median palatal notch (Fig. 4D1).

Orbital region In dorsal view, the orbital is moderately, laterally protruded (Fig. 4B). In lateral view, the orbit is large and round (Fig. 4D2). A small lacrimal orifice is present at the inner border of the anterior end of the orbital rim (Fig. 4D2, l o). Another rounded foramen passing to the nasal cavity is present at the anterior part of the orbit. It is ventral to the lacrimal orifice and dorsal to the large lacrimal bulla. A large oval opening is located at the dorsal wall of the orbit for the superior-orbital canal. The optical foramen is oval and is located at the deepest ventrocaudal corner of the orbit. The two orbital sphenoid bones on both sides are close to each other, which results in a very small distance between the optical foramina of the two sides (Fig. 4A2, of). Ventrally to the optical foramen, there is a large foramen rotundum that is concealed by the strong pterygoid process (Fig. 4D1, f ro).

Basicranial region In ventral view, the two condyles are separated by a deep and narrow notch. The posterior basilar tuberosities are separated from each other and display a prominent median groove that extends throughout the basicranium (Fig. 4A2, t pb). Compared to the posterior basilar tuberosities of *H. orientalis* (Bouvrain and de Bonis, 1988), those of *H. longdongica* are relatively weak. The basioccipital, positioned between the posterior and anterior basilar tuberosities, is elongated and exhibits a shallow depression on each side that is anterior to the anterior basilar tuberosity. The latter elements are also relatively weak and show only a slight expansion (Fig. 4A2, t ab).

The tympanic bulla is large and ellipsoidal with a pronounced ventral bulge (Fig. 4A1, A2, tb). The auditory tube is moderately long, facing laterally, and lacks a meatal fissure. The tympanohyal vagina deeply excavates the tympanic bulla and is anteriorly positioned (Fig. 4A1, A2, tv), which resembles the condition seen in living *Gazella*. However, the lamina vaginalis is poorly developed. The stylomastoid foramen is significantly separated from the tympanohyal because of the strong posterior expansion of the bulla. The petrosal bone cannot be observed because of the close contact between the tympanic bulla and the basioccipital. On the alisphenoid, there is a shallow groove anterior to the tympanic bulla that houses the Eustachian tube (Fig. 4A2, Et). The foramen ovale is relatively large (Fig. 4A2, D1, f o), and the glenoid fossa is either flat or slightly ventrally convex (Fig. 4D1, f g).

The petrosal and bony labyrinth of the type specimen GGM GSKY 22010 could not be reconstructed due to crushing. In GGM GSKY22011, the ventrolateral side of the left petrosal is exposed due to the breaking down of the tympanic bulla (the right petrosal is missing) (Fig. 4D1). The promontorium (pr) is oval and not strongly bulged, and there isn't a clearly defined

transpromontorial sulcus. The epitympanic wing is small, and its apex is relatively sharp. The cochlear fenestra (f c) is large and round. The temsor tympani (f tt), the facial sulcus (f cs), and the stapedial muscle fossa (f sm) are located in a groove that is wide and deep. The tegmen tympani is strong. Other parts are not well-preserved.

Upper check teeth (Fig. 5) The upper teeth are high-crowned. The DP2 (Fig. 5C, D) is elongated and is comprised of two lobes. The sharp paracone is the only recognizable element of this tooth. The DP3 (Fig. 5C, D) has two lobes and lacks the anterior cone. The paracone and protocone lobes are smaller than the metacone and metaconule lobes. The parastyle, mesostyle, and metastyle are all present with thin ribs. The paracone rib is thick and prominent, while the metacone rib is almost absent. The DP4 (Fig. 5C, D) shares its morphology with the upper molars, but the tooth crown is considerably lower. The parastyle and mesostyle are

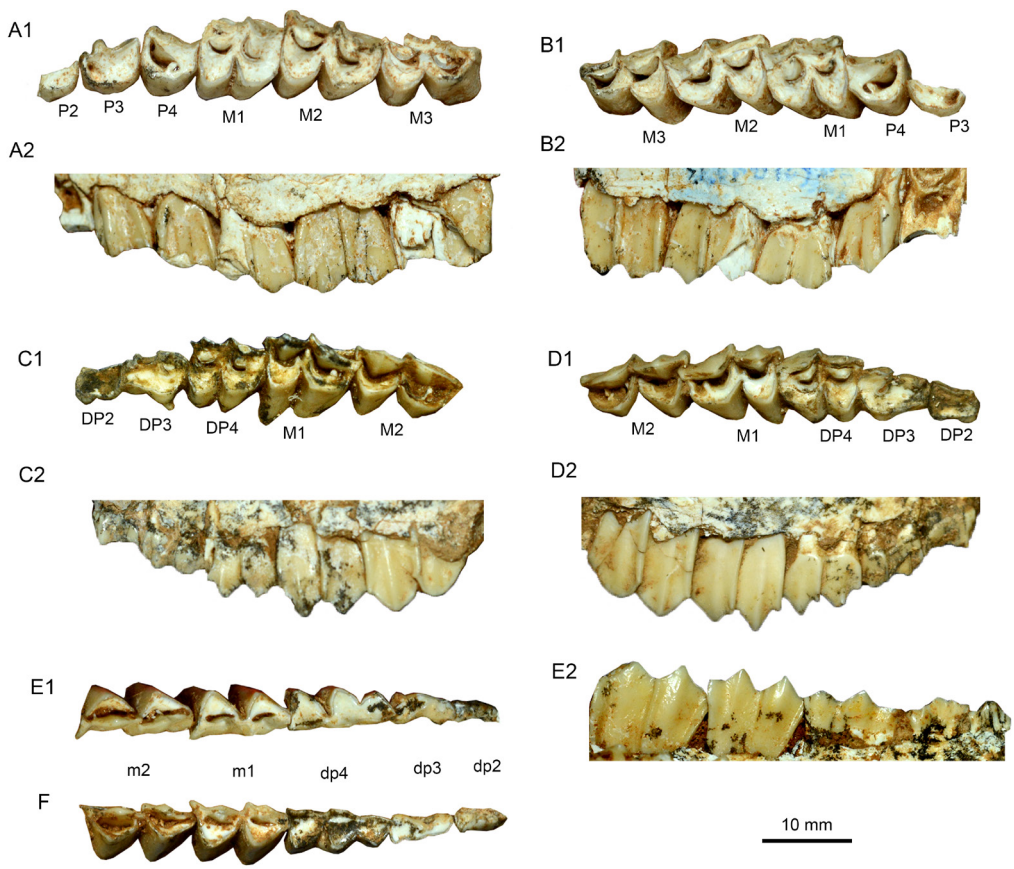

Fig. 5 Cheek teeth of *Hispanodorcas longdongica* from Daidian Locality, Qingyang
A. left upper cheek tooth row of GGM GSKY 22011, in occlusal (A1) and buccal (A2) views;
B. right upper cheek tooth row of GGM GSKY 22011, in occlusal (B1) and buccal (B2) views;
C. left upper cheek tooth row of GGM GSKY 22013, in occlusal (C1) and buccal (C2) views;
D. right upper cheek tooth row of GGM GSKY 22013, in occlusal (D1) and buccal (D2) views;
E. left lower cheek tooth row of GGM GSKY 22013, in occlusal (E1) and lingual (E2) views;
F. right lower cheek tooth row of GGM GSKY 22013, in occlusal view

prominent, featuring thin ribs, while the metastyle is comparatively weak. Similar to the DP3, the paracone rib is relatively strong and the metacone rib is weak.

The only available P2 (GGM GSKY22011) (Fig. 5A) is broken, with only the round lingula half remaining. The P3 (Fig. 5A, B) is elongated in the mediolingual direction. The lingual cone is round and exhibits a faint median groove. The labial cone has a large buccal angle with a strong rib. Both the anterior and posterior styles are weak and each have blunt ribs. Unlike the P3, the P4 (Fig. 5A, B) is not elongated and it is instead semicircular in shape. The lingual cone is round and has a very weak median groove as well. The central fold is present unless it is deeply worn. Compared to the P3, the labial cone is blunt with a relatively weak rib. However, both the anterior and posterior styles are strong, each with a prominent rib.

The M1 (Fig. 5A, B) exhibits approximately equal length and width, especially in moderately to deeply worn teeth. In occlusal view, the protocone and metaconule have relatively round lingual edges. In the slightly worn teeth, the poatprotocrista curves mesially, leaving a free end, and the premetaconulecrista contacts the buccal wall. The metaconule fold is also present. However, in the moderately to deeply worn specimens, these structures become less discernible. The paracone has a sharp buccal apex and the metacone is rather blunt. The mesostyle is strong and vertical to the buccal wall, while the para- and metastyles are relatively weak. In buccal view, both the paracone and metaconule have high and sharp apices. The ribs of the parastyle, mesostyle, and protocone are pronounced, while those of the metacone and metastyle are weak. The M2 (Fig. 5A, B) closely resembles the M1 in morphology, but it is larger and longer. The M3 (Fig. 5A, B) also has a similar structure, with the exception that the second lobe is smaller.

Mandible (Fig. 4E) Only GGM GSKY22013, the juvenile specimen, has the associated mandible. The incisor arch is broken. The diastoma between the canine and the cheek tooth row is long. The mental foramen is small and anteroposteriorly elongated. The mandible corpus is shallow and slightly bulgy, and the mandibular ramus is high and thin. The angular process is large and strongly posteriorly protruded. The condyloid process is very small.

Lower check teeth The dp2 (Fig. 5E, F) is small and simple. It has a large and high central apex, coupled with a small anterior conid and a transversely enlarged talonid-like

Table 3 Mandible mesurements of *Hispanodorcas longdongica* (GGM GSKY 22013) from Daidian Locality, Qingyang (mm)

Measurements	left/median	right
Mandible length posterior to DP2	82.0	78.3
Mandible length posterior to the tooth row	35.5	32.5
Height at the condyloid process	47.9	
Height at the mandibular notch	45.4	
Corpus height at the anterior end of DP2	12.1	12.6
Corpus height between DP4 and M1	14.3	14.9
Corpus height at the posterior end of tooth row	19.1	20.4
Length of premolar row (measured at alveoli)	14.4	16.6
Length of tooth row (measured at alveoli)	44.3	45.4

structure. The dp3 (Fig. 5E, F) closely resembles a p4 in structure, but it is more elongated. It has a substantial anterior conid and a small anterior stylid that forks from it. The mesolabial conid is inflated in the middle with a disto-oblique crest extending from it. The posterolabial conid merges with the posterolingual conid and stylid, forming a transversely enlarged complex. The dp4 (Fig. 5E, F) has three lobes, and the crown is low. Its structure is simplified due to extensive wear (known only in GGM GSKY22011). The buccal conids have relatively sharp buccal angles, while the lingual conids are nearly aligned. The metaconid is robust, and the entostylid is posteriorly oriented. A weak ectostylid is present.

In regards to the permanent lower teeth, only the m1 and m2 are known. The m1 (Fig. 5E, F) is high-crowned. In occlusal view, the protoconid and the hypoconid have relatively sharp buccal angles. The metaconid and entoconid are oblique and not aligned, but each has a relatively flattened lingual wall. The metastylid and entostylid slightly protrude distally and lingually. The ectostylid is absent. In lingual view, the metaconid and entoconid are tall and

Table 4 Tooth measurements of *Hispanodorcas longdongica* from Daidian Locality, Qingyang (mm)

			length	width	height	premolar length	molar length	total length	premolar/total
GSKY 22011	left	P2	5.3	—	4.7+				
		P3	6.6	5.3	7.4				
		P4	6.4	7.1	8.4				
		M1	9.2	8.5	6.5				
		M2	11.0	9.0	9.6+				
		M3	11.0	8.4	9.9+				
		tooth row				19.8	30.3	49.2	0.4
	right	P3	6.3	—	—				
		P4	5.0	7.5	8.2				
		M1	9.4	9.9	6.5				
		M2	10.8	9.6	10.6				
		M3	11.5	8.8	11.5				
		tooth row				—	29.7	—	—
GSKY 22013	left	DP2	6.8	4.0	4.2+				
		DP3	8.0	6.2	4.7+				
		DP4	9.3	7.9	6.9+				
		M1	11.6	8.8	12.4				
		M2	12.5	7.1	—				
	right	DP2	6.6	4.3	4.6+				
		DP3	8.3	6.2	4.9+				
		DP4	9.4	8.8	7.7				
		M1	11.6	9.9	11.2				
		M2	12.6	6.9	—				
	left	dp2	4.6	2.3	3.9				
		dp3	7.0	3.2	4.1+				
		dp4	11.0	5.0	4.7+				
		m1	11.4	5.7	10				
		m2	12.3	5.5					
	right	dp2	4.8	3.0	3.1+				
		dp3	7.1	3.2	3.6+				
		dp4	11.6	4.6	5.4+				
		m1	11.1	5.4	—				
		m2	12.2	5.8	—				

sharp, with each having a blunt rib. All the ribs of the lingual stylids are present. The m2 (Fig. 5E, F) closely resembles the m1, but it is larger, has a higher crown, and features a metaconid and entoconid that are almost aligned.

6 Comparison and discussion

The new material described in this article can be confidently attributed to *Hispanodorcas*. The key diagnostic feature of *Hispanodorcas* is the slender, posteriorly curved horncore with a 1/2 turn of homonymous twist. This feature is clearly visible in the Chinese material. The other autapomorphic features of *Hispanodorcas* (i.e., listed by Kostopoulos (2014)) are all in agreement with the Chinese material. These include the distal divergence of the horncores, the presence of a lateral groove (referred to as the laterodorsal groove in this article) that extends throughout the horncore, the absence of an anterior keel, lateral compression at the horncore base with a relatively flattened lateral surface, short pedicles, the lack of a frontal sinus, a *Gazella*-like supraorbital foramen, laterally positioned post-cornual fossae, a rostrally tapering basioccipital, and a basisphenoid with a prominent medial groove. The only distinction lies in the fact that the Chinese material features a weak flexed braincase from the facial part, which appears to be a plesiomorphic feature. This aspect will be further discussed later in the article. The Chinese material also differs from other homonymous-horncored genera in several ways. For example, it differs from *Samotragus*, *Oioceros*, and *Paraoioceros* in the lesser degree of twist of the horncore (whereas the latter three possess one or more turns of twist) (Kostopoulos, 2014). It also differs from *Sinotragus* and *Prosinotragus* in the very small size and less raised frontal bones between the horncore (Bohlin, 1935). Furthermore, it differs from *Urmiatherium polaki* and *U. rugosifronts* in the very small size and long, slender horncore (the cranial appendage of *U. intermedium* does not twist) (Kostopoulos, 2014; Shi et al., 2016).

Three species has been established within the genus *Hispanodorcas*. The type species, *H. torrubiae*, was initially discovered in Concud, Spain, MN12 of Turolian (Thomas et al., 1982). Unfortunately, no cranial material has been found. The horncores of *H. torrubiae* are notably larger and are 150%–175% longer than those of the Chinese material (Fig. 3A). Additionally, the horncores of the Chinese material have more compressed cross-sections throughout the horncore (Fig. 3A, B) and are more posteriorly bent than those of *H. torrubiae.* Moreover, a M1 has been attributed to *H. torrubiae*, which, although much larger, exhibits less developed para- and mesostyles in comparison to the Chinese material. *Hispanodorcas torrubiae* has been reported not only in various Turolian localities in Spain but also in the assemblage from the Litra Formation in Pakistan, representing the only known Asian record of *Hispanodorcas* before our discovery (Raza et al., 2002). However, the Pakistan *Hispanodorcas* has not been extensively studied.

Hispanodorcas orientalis is the second established species and was discovered from

Dytiko-3, Greece, MN13 of Turolian (Bouvrain and de Bonis, 1988). *Hispanodorcas orientalis* is smaller than *H. torrubiae* but still larger than the Chinese material in the aspect of having longer horncores and in some cranial measurements (Tables 1, 2). For example, the type horncore is 135% longer than those of the Chinese material. The horncore compression of the Chinese material is also slightly more pronounced than that of *H. orientalis* (Fig. 3A, B). The most striking differences between *H. orientalis* and the Chinese specimen include a shorter and more flexed braincase in the former, which results in a larger angle between the horncore and the cranial roof. A shorter and strongly bent braincase is typically considered as a derived feature in bovids. This, in addition to its smaller size, suggests that the Chinese material may be more primitive than *H. orientalis.* Furthermore, the Chinese material also has a thinner basioccipital bone with weaker anterior and posterior tuberosities. This is in contrast to *H. orientalis*, which exhibits a stronger and more specialized morphology of the basioccipital bone. In the cheek teeth in the Chinese material, enamel stripes are absent, and the styles and stylids appear to be stronger compared with those of *H. orientalis*. However, the teeth sizes are similar between *H. orientalis* and the Chinese materials (Fig. 3C).

Kostopoulos (2014) attributed some cranial and horncore fragments as well as lower teeth to *Hispanodorcas* cf. *H. orientalis*, which were previously identified as *Oioceros* and ?*Gazella*, from Nikiti-1, Greece, MN10 of Vallesian. This maybe be similar in age to the Daidian locality where the Chinese material was found. *Hispanodorcas* cf. *H. orientalis* appears to be more closely related to the Chinese material in terms of size, and it may have a less flexed braincase from the face. However, in lateral view, the horncore of *H.* cf. *H. orientalis* is straight, whereas those of the Chinese material are more posteriorly curved. As a result, we regard them as different species. However, more complete specimens of *Hispanodorcas* cf. *H. orientalis* are needed to confirm this assertion. Nonetheless, *Hispanodorcas* cf. *H. orientalis* and the Chinese material are likely closely related and together represent the more primitive members of the genus.

A third species is *H. heintzi*, discovered in La Calera, Spain, MN14 of Rucinian (Alcalá and Morales 2006). This species represents the latest and most derived member of the genus. It differs significantly from the Chinese material in several ways. *H. heintzi* is notably larger (Fig. 3), and its horncores feature anterior and posterior keels, while the laterodorsal groove is either weak or absent. As the Chinese material exhibits distinct differences from all unequivocal species of *Hispanodorcas*, we have established a new species, *H. longdongica*. This discovery marks the first and only known occurrence of *Hispanodorcas* in China and East Asia.

Apart from the previously mentioned species, there are several other materials that have been associated with *Hispanodorcas*. Firstly, *Samotragus pilgrimi* from Toril 3, Spain, MN7/8 of the Middle Miocene (Azanza et al., 1998) was attributed to ?*Hispanodorcas* by Kostopoulos (2014). We have also recently discovered a homonymous twisted horncore that resembles

?*Hispanodorcas pilgrim* from the Halamagai Formation (~17–15 Ma), China (unpublished data). Although Kostopoulos (2014) pointed out many features that are reminiscent of *Hispanodorcas*, he also noted that the thicker and shorter horncores, as well as the deep braincase of ?*Hispanodorcas pilgrimi*, differ from those of other *Hispanodorcas* species. Indeed, it is possible that ?*Hispanodorcas pilgrimi* might belong to *Hispanodorcas*. However, it could also be possible that ?*Hispanodorcas pilgrimi* represents another (new) genus that is not closely related to *Hispanodorcas*. Particularly, the molars of ?*Hispanodorcas pilgrim* display a relatively strong ecto-/entostylis (at least in m1 and m2, see Azanza et al. 1998:fig. 1) that is totally absent in the other known species of *Hispanodorcas*.

"*Gazella*" *rodleri* Pilgram and Hopwood, 1928 is another taxa that was frequently mentioned when discussing *Hispanodorcas*. It was attributed to *Hispanodorcas* by Gentry and Heizmann (1996) in question. However, as Kostopoulos and Bernor (2011) pointed out that "*Gazella*" *rodleri* possesses a thick horncore with a very weak twist (~1/4 turn). The frontal bone is thickened with the initial development of the sinus system. Kostopoulos and Bernor (2011) suggested that "*Gazella*" *rodleri* is more likely a caprine rather than an antilopine and established the genus *Demecquenemia* for this taxon, renaming it *D. rodleri.* We agree with this opinion. In the Late Miocene of China, similar specimens were also reported, such as Antilope gen. et sp. indet. or *Olonbulukia* sp. from the Qaidam Basin (Bohlin, 1937; Wang et al., 2019), which warrant further study.

Thomas et al. (1982) mentioned a specimen (THP 29.405) from Yushe, China, first reported by Teilhard de Chardin and Trassart (1938). Thomas et al. (1982) suggested that it might phylogenetically connect to *Hispanodorcas*. Although the Yushe specimen displays a weak homonymous twist (less than 1 turn) of the horncore akin to that in *Hispanodorcas*, the two horncones insert very closely to each other and strongly converge in the proximal half. This is distinct from *Hispanodorcas*, in which the two horncores insert very distantly and do not converge proximally. In these aspects, the Yushe specimen is morphologically close to the specimens attributed to "*Oioceros* sp." (or more probably, "*Samotragus* sp.") from the Pliocene localities of Lingtai, Gansu (unpublished data), except for in the less homonymous twisted horncore. Nevertheless, a more detailed study of the morphology of these "*Oioceros*"-like specimens should be conducted in the future. Here, we do not consider the Yushe specimen to be closely related to *Hispanodorcas*.

The next question pertains to which tribe *Hispanodorcas* should be assigned. Obviously, it belongs to the Antilopinae, not the Bovinae. Within the Antilopinae, there are three hypotheses: Antilopini, Reduncini, and Oiocerini. Thomas et al. (1982) excluded it from Reduncini due to the absence of frontal bones raised for holding the frontal sinus. Furthermore, the cheek teeth of *Hispanodorcas* exhibit clear aegodont characteristics, unlike the boodont teeth found in reduncines.

Kostopoulos (2014) grouped *Hispanodorcas* with those taxa possessing homonymous spiral or twisted horncores and attributed them to Oiocerini. However, the question of whether Oiocerini truly constitutes a monophyletic group is debatable. Homonymous horncores are a rare characteristic among living bovids, but they were not uncommon in the Late Miocene bovids. In this discussion, we exclude the Early to Middle Miocene taxa, like *Turcocerus*. For the Late Miocene taxa such as *Samotragus*, *Oioceros*, and *Paraoioceros* from Greece, and *Shanxispira* from China, these typical oiocerines have homonymous horncores with more than one full turn (Kostopoulos, 2014; Shi et al., 2014). They are typically relatively large and possess raised frontal bones for the development of the frontal sinus. The braincase is usually short and strongly flexed, and the horncores are typically thicker. These features differ from those of *Hispanodorcas*. It should be noted that the development of the frontal and horncore sinuses, the short and flexed brain case, and the thick horncores point to the tribe Caprini. Therefore, those typical oiocerine taxa (*Samotragus*, *Oioceros*, *Paraoioceros*, *Shanxispira*, etc.) might represent a group within Caprini. However, *Hispanodorcas* does not fit this profile. All species of *Hispanodorcas* are small and not any larger than living *Gazella*. *Hispanodorcas longdongica* is even smaller than any living or fossil *Gazella*. The horncores are slender, and the frontal and horncore sinuses are absent. The braincase is relatively long and resembles that of *Gazella*. In *H. longdongica*, the braincase is poorly flexed, which is akin to the condition in *Gazella*. The homonymous rotation of the horncores, which might have evolved in parallel with that of oiocerines, however, is very weak and only reaches around a 1/2 turn. Therefore, *Hispanodorcas* might represent a group derived from the "*Gazella* stock." This assertion was also made by Bouvrain and de Bonis (1988). However, based on molecular data, the previously defined Antilopinae (sensu Simpson (1945)) is not a monophyletic group. When considering various fossil "*Gazella*" and *Gazella*-like taxa, determining the phylogenetic position of *Hispanodorcas* remains a challenging problem. Nevertheless, the presence of *H. longdongica* provides further evidence for the existence of a continuous savanna-like biome between the eastern and western parts of the mid-latitude zone of Eurasia that resulted in a high faunal similarity along this corridor during the Late Miocene (Kaya et al., 2018).

7 Conclusion

In this article, we present the first-known species of *Hispanodorcas* from the Late Miocene of China, known as *Hispanodorcas longdongica*. This species is the smallest amongst the genus and exhibits several primitive features, such as a weak bend in the braincase from the facial region and the presence of weak anterior and posterior basilar tuberosities. Therefore, *H. longdongica* may represent an early evolutionary stage of this genus. The age of this discovery has been correlated with the early Baodean period based on the mammalian assemblage, particularly due to the presence of *Hipparion hippidiodus* and *Hi. coelophyes.* The discovery

of this new species expands our understanding of the distribution of *Hispanodorcas*, which is an extremely intriguing animal. It also suggests that *Hispanodorcas* may be phylogenetically closer to the "*Gazella* stock" rather than it possibly being attributed to the caprine-related Oiocerini.

Acknowledgements We thank Jie Ye, Chunxiao Li, and Danhui Sun, Institute of Vertebrate Paleontology and Paleoanthropology, China; Yikun Li, Shenyang Normal University, China; Yonggang Liu, Lei Zhang, Department of Natural Resources of Gansu Province, China; Tingwei Li, Yongqiang Nan, Xinming Zhang, Feihong Guo, Qingyang Bureau of Natural and Resources, China; Yan Li, Gansu Provincial Museum, China; Cuo Peng, Lingqi Zhou, Gansu Geological Museum, China; Daqing Li, Jingtao Yang, Gansu Agricultural University, China; Shuang Dai, Lanzhou University, China; Jiwei Liang, Chang'an University, China, for participating in this work. The work was supported by the National Key Research and Development Program of China (No. 2023YFF0804500), the Second Tibetan Plateau Scientific Expedition (2019QZKK0705), and the Fossil Protection Project issued by the Department of Natural Resources of Gansu Province, China.

中国首次发现晚中新世西班牙羚(*Hispanodorcas*)

吴　勇[1]　王世骐[2]　梁志勇[1]　郭丁歌[2,3]　孙博阳[2]
刘　龙[1]　段　凯[1]　陈国忠[1]

(1 甘肃省地质矿产勘查开发局第三地质矿产勘查院 兰州 730050)

(2 中国科学院古脊椎动物与古人类研究所，中国科学院脊椎动物演化与人类起源重点实验室 北京 100044)

(3 中国科学院大学 北京 100049)

摘要：西班牙羚(*Hispanodorcas*)是一类中小型牛科动物，此前只在泛地中海地区和南亚有所发现。西班牙羚的分类一直有所争议，曾被认为与羚羊族(Antilopini), 苇羚族(Reduncini)或角羊族(Oiocerini)有关。报道了在中国庆阳正宁地区的代店化石点首次发现的陇东西班牙羚新种(*H. longdongica* sp. nov.), 时代大约为早保德期(约8–7百万年前)。新材料包括5个头骨，保存状态各异，提供了迄今为止关于西班牙羚最完整的骨骼信息。其角心长而细、向后弯曲，且微弱地同向扭曲(homonymous twist); 角心同时还具有和外–背侧沟和内–腹沟，这些都是西班牙羚的典型特征。代店地点发现的西班牙羚在已知各种中体型最小，面部和脑颅之间的弯曲较弱，前后基结节均发育较弱。这些原始的特征表明陇东西班牙羚可能代

表了这个属的早期演化阶段。此外，该种头骨与瞪羚(*Gazella*)的相似之处表明西班牙羚可能是直接从瞪羚的祖先演化而来，其同向扭转的角心与角羊族一致，可能是两者平行演化所致。

关键词：庆阳，东亚，保德期，羚羊族，三趾马动物群，西班牙羚

References

Alcalá L, Morales J, 2006. Antilopinae (Bovidae, Mammalia) from the Lower Pliocene of Teruel Basin (Spain). Estud Geol, 62(1): 559–570

Azanza B, Nieto M, Morales J, 1998. *Samotragus pilgrimi* n. sp., a new species of Oiocerini (Bovidae, Mammalia) from the Middle Miocene of Spain. C R Acad Sci Ser IIA Earth Planet Sci, 326(5): 377–382

Bärmann E V, Rössner G E, 2011. Dental nomenclature in Ruminantia: towards a standard terminological framework. Mammal Biol, 76: 762–768

Bärmann E V, Wronski T, Lerp H et al., 2013. A morphometric and genetic framework for the genus *Gazella* de Blainville, 1816 (Ruminantia: Bovidae) with special focus on Arabian and Levantine Mountain gazelles. Zool J Linn Soc, 169: 673–696

Bohlin B, 1935. Cavicornier der *Hipparion*-Fauna Nord-Chinas. Palaeontol Sin Ser C, 9(4): 1–166

Bohlin B, 1937. Eine tertiäre Saugetier-Fauna aus Tsaidam. Palaeontol Sin Ser C, 14(1): 1–111

Bouvrain G, de Bonis L, 1988. Découverte du genre *Hispanodorcas* (Bovidae, Artiodactyla) dan le turolien de Grèce septentrionale. Ann Paléontol, 74(2): 97–112

Flynn L J, Deng T, Wang Y et al., 2011. Observations on the *Hipparion* Red Clays of the Loess Plateau. Vert PalAsiat, 49(3): 275–284

Gentry A, Heizmann E P J, 1996. Miocene ruminants of central and eastern Tethys and Paratethys. In: Bernor R, Fahlbush V, Mittmann H W eds. The Evolution of Western Eurasian Neogene Mammal Faunas. New York: Columbia University Press. 378–391

Gray J E, 1821. On the natural arrangement of vertebrose animals. Lond Med Rep Month J Rev, 15: 296–310

Kaya F, Bibi F, Žliobaitė I et al., 2018. The rise and fall of the Old World savannah fauna and the origins of the African savannah biome. Nat Ecol Evol, 2: 241–246

Kostopoulos D S, 2014. Taxonomic re-assessment and phylogenetic relationships of Miocene homonymously spiral-horned antelopes. Acta Palaeontol Pol, 59(1): 9–29

Kostopoulos D S, Bernor R L, 2011. The Maragheh bovids (Mammalia, Artiodactyla): systematic revision and biostratigraphic-zoogeographic interpretation. Geodiversitas, 33(4): 649–708

Pilgram G M, Hopwood A T, 1928. Catalogue of the Pontian Bovidae of Europe. London: British Museum (Natural History). 1–106

Raza S M, Cheema I U, Downs W R et al., 2002. Miocene stratigraphy and mammal fauna from the Sulaiman Range, Southwestern Himalayas, Pakistan. Palaeogeogr Palaeoclimatol Palaeoecol, 186: 185–197

Shi Q Q, He W, Chen S Q. 2014. A new species of *Shaanxispira* (Bovidae, Artiodactyla) from the upper Miocene of China. Zootaxa, 3794(4): 501–513

Shi Q Q, Wang S Q, Chen S K et al., 2016. The first discovery of *Urmiatherium* (Bovidae, Artiodactyla) from Liushu Formation, Linxia Basin. Vert PalAsiat, 54(4): 319–331

Simpson G G, 1945. The principles of classification and a classification of mammals. Bull Am Mus Nat Hist, 85: 1–350

Sun B Y, 2018. Systematic revision, phylogenetic analysis on Chinese fossil horse of Equinae and discussion on their evolution, migration and environment setting. Ph. D thesis. Beijing: University of Chinese Academy of Sciences. 1–167

Sun B Y, in press. Fossil Equidae in the Linxia Basin with biostratigraphic and paleozoogeographic significance. Acta Geol Sin-Engl. https://doi.org/10.1111/1755-6724.15097

Sun J M, Ding Z L, Xiao W J et al., 2022. Coupling between uplift of the Central Asian Orogenic Belt-NE Tibetan Plateau and accumulation of aeolian Red Clay in the inner Asia began at ~7 Ma. Earth Sci Rev, 226: 103919

Teilhard de Chardin P, Trassaert M, 1938. Cavicornia of south-eastern Shansi. Palaeontol Sin, New Ser C, 6: 1–98

Thomas H, Morales J, Heintz E, 1982. Un nouveau bovidé (Artiodactyla, Mammalia), *Hispanodorcas* torrubiae n. g., n. sp., dans le Miocene Supérieur d'Espagne. Mus Nat d'Hist Nat, 4: 209–222

Wang S Q, Yang Q, Zhao Y et al., 2019. New *Olonbulukia* material and its related assemblage reveal an early radiation of stem Caprini along the north of the Tibetan Plateau. J Paleontol, 93(2): 385–397